

1
2
3
4
5
6
7
8
9
10
11
12
13
14
15
16
17
18
19
20
21
22
23
24
25
26

Distinct roles for phosphoinositide 3-kinases γ and δ in malignant B cell migration

Ahmed Y. Ali^{1,3}, Xun Wu¹, Nour Eissa¹, Sen Hou¹, Jean-Eric Ghia^{1,2}, Thomas T. Murooka^{1,3}, Versha Banerji^{4,5}, James B. Johnston⁴, Francis Lin^{1,6}, Spencer B. Gibson^{1,4,5}, Aaron J. Marshall^{1,4,5,7}

¹ Department of Immunology, University of Manitoba
² Department of Internal Medicine, Section of Gastroenterology, University of Manitoba
³ Department of Medical Microbiology and Infectious Diseases, University of Manitoba
⁴ Research Institute in Oncology and Hematology, CancerCare Manitoba
⁵ Department of Biochemistry and Medical Genetics, University of Manitoba
⁶ Department of Physics and Astronomy, University of Manitoba

⁷ Correspondence to: Dr. Aaron Marshall, Department of Immunology, University of Manitoba, 750 McDermot Avenue, Winnipeg, MB, Canada, R3E-0T5.

Running title: Unique functions of PI3K γ in B cell malignancy

27 **Key Points**

28 • PI3K γ has unique non-redundant functions in malignant B cell migration and adhesion to
29 stromal cells

30

31 • Targeting both PI3K γ and PI3K δ can have a greater impact on chemokine-dependent
32 responses than targeting either isoform alone

33

34

35

36

37 **Abstract**

38 The PI 3-kinases (PI3K) are essential mediators of chemokine receptor signaling necessary for
39 migration of chronic lymphocytic leukemia (CLL) cells and their interaction with tissue-resident
40 stromal cells. While the PI3K δ -specific inhibitor idelalisib shows efficacy in treatment of CLL
41 and other B cell malignancies, the function of PI3K γ has not been extensively studied in B cells.
42 Here we assess whether PI3K γ has non-redundant functions in CLL migration and adhesion to
43 stromal cells. We observed that pharmaceutical PI3K γ inhibition with CZC24832 significantly
44 impaired CLL migration, while dual PI3K δ/γ inhibitor duvelisib had a greater impact than single
45 isoform-selective inhibitors. Knockdown of PI3K γ reduced migration of primary CLL cells and
46 cell lines. Expression of the PI3K γ subunits increased in CLL cells in response to CD40L/IL-4,
47 whereas BCR cross-linking had no effect. Overexpression of PI3K γ subunits enhanced cell
48 migration in response to SDF1 α /CXCL12, with the strongest effect observed within ZAP70⁺
49 CLL samples. Microscopic tracking of cell migration within chemokine gradients revealed that
50 PI3K γ functions in gradient sensing and impacts cell morphology and F-actin polarization.
51 PI3K γ inhibition also reduced CLL adhesion to stromal cells to a similar extent as idelalisib.
52 These findings provide the first evidence that PI3K γ has unique functions in malignant B cells.

53

54 **Introduction**

55 Chronic Lymphocytic Leukemia (CLL) is a prevalent hematologic malignancy affecting adults
56 in the West. CLL cells rely on chronic activation triggered via the B-cell receptor (BCR) to
57 potentiate their survival (1). Within lymphoid tissues, CLL cells interact with and shape a
58 microenvironment favourable to their survival and proliferation (2). They migrate to favourable
59 niches in response to chemotactic factors, such as the chemokine stromal-derived factor 1
60 (SDF1 α). They interact with resident stromal cells that provide them with survival and
61 proliferative stimuli through cell-cell contact and soluble factors (3-5). The protective
62 microenvironment shields CLL cells from the effects of therapeutics, conferring a resistant
63 phenotype.

64

65 CLL varies from indolent to progressive forms according to the expression of several
66 biomarkers, immunoglobulin variable heavy chain (IgVH) mutation, and chromosomal
67 abnormalities (6, 7). One such biomarker is the expression of zeta-chain T-cell receptor-
68 associated protein kinase 70 kDa (ZAP70) (8, 9). We and others have shown that ZAP70
69 expression can alter CLL adhesion and migration (10-12); however, the mechanisms for this
70 remain unclear.

71

72 The phosphoinositide-3 kinase (PI3K) signaling pathway has been implicated in numerous
73 malignancies (13-17). PI3K enzymes phosphorylate the 3' hydroxyl group of the inositol ring of
74 phosphoinositide lipids. PI3K δ has established functions in normal and malignant B cell
75 signaling, and the p110 δ -specific inhibitor idelalisib has been effective in CLL treatment (18,

76 19). Inhibition of PI3K δ affects multiple aspects of CLL biology including cell adhesion and
77 migration in response to chemokines (20, 21).

78

79 PI3K γ consists of a catalytic subunit (p110 γ) and one of two regulatory subunits (p84 or p101)
80 which bind to p110 γ and have different effects on p110 γ activity in terms of cellular migration
81 (22, 23). PI3K γ is recruited to activated chemokine receptors via p101-dependent binding to
82 G β / γ subunits (24-26), whereas the mechanism of PI3K δ activation by chemokines is unclear.
83 PI3K γ has well-established functions in T lymphocyte and neutrophil chemokine receptor
84 signaling, but has not been extensively studied in B lymphocytes (27, 28). In fact, the limited
85 data available on B cell function in PI3K γ -deficient mice indicate that this enzyme is not
86 essential for B cell activation or migration (29, 30). Despite this, PI3K γ inhibitors are now in
87 clinical development for B cell malignancies (31).

88

89 In this study, we present our novel findings that PI3K δ and PI3K γ have unique, non-redundant
90 functions in CLL cell migration and adhesion to stromal cells. These findings indicate that
91 targeting PI3K γ alone or in combination with PI3K δ may have a unique impact on CLL biology
92 with potential therapeutic benefit.

93

94 **Materials and Methods**

95 *CLL cells and cell lines*

96 CLL cells were isolated from peripheral blood samples using RosetteSep Human B Cell
97 Enrichment Cocktail (StemCell Technologies) at CancerCare Manitoba with the approval of the
98 Research Ethics Board at the University of Manitoba. ZAP-70 and IgVH mutation status were
99 determined as previously described (32). Patient characteristics are described in **Table S1**. in
100 CLL-derived JVM3 and Burkitt lymphoma Ramos cells were obtained from DSMZ, Germany.
101 HS-5 human bone marrow-derived stromal cells were obtained from ATCC. All cells were
102 grown in RPMI1640 media supplemented with 10% fetal bovine serum and 1% penicillin-
103 streptomycin (GIBCO).

104 *Chemicals and Reagents*

105 PI3K inhibitors CZC24832, GS-1101/idelalisib, IPI-145/duvelisib, and GDC-0980/apitolisib
106 (Selleck Chemicals) were reconstituted in DMSO (Sigma) and used at a final concentration of 2
107 μM (CZC24832) and 1 μM (idelalisib, duvelisib, GDC-0980). CZC24832 has greater than 10-
108 fold selectivity over PI3K β and greater than 100 selectivity over PI3K α and PI3K δ (33). α -IgM
109 F(ab')₂ (Southern Biotech) was used at 10 $\mu\text{g}/\text{ml}$ and CD40 ligand and interleukin 4 (R&D
110 systems) were used at 50 ng/ml each. Anti-p110 γ antibody (R&D systems), anti-GAPDH
111 antibody (Cell Signaling), and Mini-PROTEAN TGX precast gels (Bio-Rad) were used for
112 Western blot analysis. SDF1 α (Peprotech) was used at 100 ng/ml. Alexa Fluor® 488 Phalloidin
113 (Life Technologies) was used at 33 nM for F-actin staining. Superscript VILO cDNA mix

114 (Invitrogen) was used for RT-qPCR. DAPI, trypsin-EDTA (Sigma), and anti CD19-FITC
115 antibody (BD Biosciences) were used for the cell adhesion assay.

116 *Western blotting*

117 The experiments were performed as previously described (34). Membranes were incubated
118 overnight at 4° C with anti-p110 γ and anti-p101 antibodies (1:1000 dilution). GAPDH served as
119 a loading control (1:10,000 dilution). HRP-conjugated anti-rabbit (Cell Signaling) and anti-
120 mouse (Jackson Immunoresearch) secondary antibodies (1:5000 dilution) were used for
121 chemiluminescent detection.

122 *Real-time Quantitative PCR*

123 The experiments were performed as previously described (35). Briefly, 5 million CLL cells per
124 treatment group were stimulated for 24 hours with α -IgM or CD40L/IL-4, collected in TRIzol,
125 and total RNA was isolated and purified using the Purelink RNA kit (Thermo Fisher). qPCR was
126 performed using a LightCycler 96 PCR instrument (Roche Diagnostics) and Power SYBR green
127 (Applied Biosystems). All reactions were run in duplicates (primer sequences available in **Fig**
128 **S1A**).

129 *Plasmid constructs*

130 Expression vectors for p110 γ -GFP or p101-GFP used the pLenti-GIII-CMV-GFP-2A-Puro
131 backbone (Applied Biological Materials). The expression vector for dCas9-GFP is pLV-hUbc-
132 dCas9-T2A-GFP (Addgene #53191). Guide RNA expression cassettes targeting the p110 γ gene
133 were designed based on a CRISPRi optimized gRNA sequence library (36) and synthesized by
134 Integrated DNA Technologies (sequences in **Fig S1B**). gRNA cassettes were cloned into the

135 XbaI/XhoI sites of vector pU6-sgRNA EF1Alpha-puro-T2A-BFP (Addgene #60955) for use in
136 CRISPRi (**Fig S1B**). For CRISPRi experiments, the two p110 γ gRNA plasmid vectors were
137 mixed with dCas9-GFP plasmid at a 3:1 ratio (gRNA:dCas9) for transfection.

138 *Cell transfection*

139 For cell lines, 5×10^5 cells were transfected with each plasmid (1 μ g) using the Neon Transfection
140 system (Invitrogen), using the following condition: JVM3 1200 V, 20 ms, 2 pulses; Ramos 1600
141 V, 20 ms, 1 pulse. For primary CLL cells, 1×10^6 cells were transfected with each plasmid (2.5
142 μ g) using 2250 V, 20 ms, 1 pulse. Transfection efficiency was 20-30% for cell lines and 8-12%
143 for primary CLL as assessed by GFP expression.

144 *Transwell Migration and Adhesion Assays*

145 The experiments were performed as previously described (32, 37). Migration assays used
146 Corning transwell plates containing 5×10^5 cells and 8 μ m insert (cell lines) and 1×10^6 cells and 5
147 μ m insert (CLL), and SDF1 α (3h). Adhesion assays used 5×10^4 HS-5 cells/well and 5×10^6
148 primary CLL cells/well (24h). Migrated/non-migrated fractions and adhered/non-adhered
149 fractions were collected and counted by flow cytometry gating on live B cells.

150 *Microscopy-based Chemokinesis and Chemotaxis Assays*

151 For chemokinesis assays, μ -Slide 8 well chamber slides (Ibidi) were coated with 1 μ g/ml
152 VCAM-1 at 4 $^{\circ}$ C overnight and washed with warm RPMI1640. 1×10^5 Ramos cells were added to
153 allow adhesion (0.5h), then incubated with the inhibitors (0.5h) in serum-free medium. After
154 adding SDF1 α , migration was assessed by time-lapse imaging. For chemotaxis assays, μ -Slide
155 Chemotaxis^{3D} chambers were pre-warmed to 37 $^{\circ}$ C prior to addition of cell/collagen mixtures.

156 Collagen gel mixtures (1.7 mg/ml) were made using PureCol Bovine Collagen (Advanced
157 Biomatrix) and kept on ice (38). JVM3 cells (3×10^6 /mL) and inhibitors were added, and the
158 mixture was loaded into chambers. Cell migration was recorded by Zeiss AxioObserver confocal
159 microscope equipped with environmental control (37°C, 5% CO₂).

160 *Cell Tracking and Data Analysis*

161 Movement of individual cells, tracked using IMARIS 8.0 software, was quantitatively evaluated
162 by (1) Chemotactic Index [ratio of the displacement of cells toward the chemokine gradient (Δy)
163 to the total migration distance (d) using the equation $C.I. = \Delta y/d$, presented as the average value
164 \pm standard error of the mean (SEM)]; (2) average cell migration speed ($d/\Delta t$; average value \pm
165 SEM of all cells). (3) Magnitude of velocity (track displacement/ Δt). (4) Mean Square
166 Displacement plots cell displacement as a function of time as a measure of migration persistence.

167 *Intracellular Staining, Morphological Scoring and Confocal Microscopy*

168 Ramos cells were added to VCAM-1-coated chamber slides to allow adhesion (0.5h) then
169 incubated with the inhibitors (0.5h) in serum-free medium. Cells were then stimulated (SDF1 α)
170 for the indicated time, fixed (2% PFA), permeabilized (0.5% saponin), washed and stained for F-
171 actin using Alexa Fluor 488 phalloidin (Life Technology). Images were taken by Zeiss
172 AxioObserver confocal microscope under 63 \times magnification.

173 *Statistical Analysis*

174 Unless indicated otherwise, Student's t test was used to calculate statistical significance ($*p$
175 <0.05 , $**p <0.01$, $***p <0.001$). Error bars represent SEM.

177 **Results**

178

179 **Inhibition of PI3K γ impairs cell migration to a similar extent as PI3K δ inhibition.**

180 Inhibition of PI3K δ impairs malignant B cell adhesion and migration (32, 39); however, the role
181 of PI3K γ in this context is unknown. To assess the roles of each PI3K isoform in the regulation
182 of CLL cell migration, we have used isoform-specific inhibitors CZC24832 (PI3K γ -specific),
183 GS-1101/idelalisib (PI3K δ -specific), and dual PI3K δ /PI3K γ inhibitor IPI-145/duvelisib. Pan-
184 PI3K inhibitor GDC-0980/apitolisib was used as a positive control. JVM3 cells, maintained in
185 medium or stimulated for 24 hours with CD40L/IL-4, were pre-incubated (1h) with CZC24832,
186 idelalisib, duvelisib, or GDC-0980. Migration capacity was assessed using a transwell chambers
187 containing SDF1 α in the bottom chamber and the inhibitors in both top and bottom chambers to
188 ensure continued inhibition during the assay. We found that PI3K γ inhibition significantly
189 reduced the migration of stimulated JVM3 cells to similar extent as PI3K δ inhibition (**Fig 1A**).
190 Dual PI3K δ /PI3K γ inhibition further decreased JVM3 cell migration to a level comparable to
191 pan-PI3K inhibition (**Fig 1A**). Western blot analysis revealed that CZC24832 reduced SDF1 α -
192 induced phosphorylation of Akt in a dose-dependent manner (**Fig 1B**).

193 We then assessed the sensitivity of CLL cell migration to these inhibitors under the same
194 conditions and observed that PI3K γ inhibition alone is sufficient to significantly decrease CLL
195 cell migration, with or without CD40L/IL-4 pre-stimulation (**Fig 2A-C**). PI3K γ or PI3K δ
196 inhibitors reduced CLL migration to a similar extent, whereas dual inhibition with duvelisib had
197 a significantly greater impact on migration than PI3K γ inhibition alone (**Fig 2A-B**). Moreover,
198 the combination of CZC24832 and idelalisib had a significantly greater effect on CLL migration
199 that either inhibitor alone (**Fig 2C**). Grouping CLL patients based on major prognostic markers

200 showed that PI3K γ inhibition sensitivity was similar in progressive and indolent disease groups
201 defined by ZAP70 or IgVH mutation status (**Fig S2**). Consistent with these functional data,
202 PI3K γ inhibition reduced phosphorylation of Akt and its downstream targets GSK3 β and S6
203 kinase in CLL cells and greater inhibition was observed with dual PI3K δ /PI3K γ inhibition (**Fig**
204 **S3A**). Inhibitor treatments did not affect relative expression of different PI3K isoforms (**Fig**
205 **S3B**) or cell viability (**Fig S4**). Migration of normal human B cells was also significantly
206 impaired by idelalisib, duvelisib and GDC-0980, whereas PI3K γ inhibitor had a relatively small
207 effect which did not reach statistical significance (**Fig S5**). Together these results provide the
208 first demonstration that PI3K γ has a non-redundant role in CLL cell migration, and suggest that
209 combined PI3K γ and PI3K δ targeting may in some contexts have a greater impact than targeting
210 either isoform alone.

211

212 **Knockdown of p110 γ significantly reduced CLL cell migration.**

213

214 We employed CRISPRi technology to provide an independent means of assessing the importance
215 of PI3K γ in CLL cell migration. Two guide RNAs were designed targeting different sites of the
216 p110 γ gene, and co-expressed with dCas9-GFP in malignant B cell lines Ramos and JVM3. This
217 method was sufficient to significantly and specifically reduce p110 γ expression as determined by
218 qPCR analysis of p110 subunit expression (**Fig 3A and Fig S6A**). Following a 48h recovery
219 period, transfected cells were assessed for migration using a transwell assay. We observed that
220 p110 γ downregulation significantly reduced cell migration compared to control cells (**Fig 3B**).
221 Moreover, knockdown of p110 γ in primary CLL cells significantly reduced their migration
222 independently of IgVH mutation status (**Fig 3C**) and ZAP70 expression (**Fig S6B**), without

223 compromising cell viability (**Fig S4B**). These results are consistent with those seen with PI3K γ
224 inhibition, and confirm that PI3K γ has an independent and essential function in malignant B cell
225 migration.

226

227 **Expression of PI3K γ in CLL is enhanced in response to CD40L/IL-4 stimulation**
228 **independently of ZAP70 status or IgVH mutation.**

229 We examined the expression of PI3K γ subunits in CLL prognostic groups and determined
230 whether PI3K γ expression is influenced by BCR cross-linking or stimulation with T cell-derived
231 factors. Purified CLL cells were stimulated (24 h) with α -IgM or CD40L/IL-4 and mRNA
232 abundance of p110 γ and p101 were determined. We observed that the expression of p110 γ
233 mRNA was significantly upregulated after CD40L/IL-4 stimulation, but not after α -IgM
234 stimulation, regardless of ZAP70 or IgVH mutation status (**Fig 4A and Fig S7A**). Both α -IgM
235 and CD40L/IL-4 stimulation were able to activate the PI3K kinase signaling pathway in CLL
236 (**Fig S8**). Expression of p101 was highly heterogeneous, but the majority of CLL patients
237 showed increased p101 expression after CD40L/IL-4 stimulation (**Fig 4B and Fig S7B**).
238 Interestingly, a few patients who expressed p101 at high levels without stimulation showed the
239 reverse trend (**Fig S7B**), suggesting that distinct mechanisms may maintain high p101 expression
240 in these patients. Examination of p110 γ and p101 protein expression also indicated
241 heterogeneity and a trend of increased expression after CD40L/IL-4 stimulation (**Fig 4C**).
242 Analysis of microarray data generated from leukemic B cells isolated from CLL patient
243 peripheral blood or lymph nodes [GEO dataset GDS4176; (40)] revealed that both p110 γ and
244 p101 are more highly expressed in lymph node than peripheral blood (**Fig S9**). Together these

245 results indicate that CLL cells express PI3K γ and its expression can be modulated by factors
246 present in the lymphoid tissue microenvironment.

247

248 **Overexpression of PI3K γ enhances chemokine-induced cell migration.**

249 To determine whether increased PI3K γ expression can impact the migration of CLL cells, p110 γ
250 or p101 subunits were each expressed in JVM3 cells. After transfection with either p110 γ -GFP
251 or p101-GFP expression plasmids, overexpression was confirmed by qPCR (**Fig 5A**). Migration
252 of the transfected cells was measured using the transwell assay. We found that chemokine-
253 induced migration of JVM3 cells is significantly increased by overexpression of either p110 γ or
254 p101 (**Fig. 5B**). We further determined the impact of PI3K γ subunits on migration of CLL cells.
255 While expression of p101 did not increase CLL migration, expression of p110 γ resulted in
256 significant but variable increases in migration (**Fig 5C**). Co-expression of both p110 γ and p101
257 significantly increased migration in the majority of CLL patient samples, and had a significantly
258 greater impact than expression of p110 γ alone (**Fig 5C**). Together these data support the
259 importance of PI3K γ in CLL migration and suggest that its expression level is an important
260 factor determining cellular migration capacity.

261

262 **Impact of PI3K γ or PI3K δ inhibition on migration behavior within chemokine gradients**

263 Unlike PI3K δ , PI3K γ is known to directly associate with G-protein coupled receptors via binding
264 to activated G β / γ subunits (25, 41) and can mediate directional migration within chemokine
265 gradients (29, 30, 42). To determine whether PI3K γ and PI3K δ may affect distinct migration
266 behaviors, cells were observed by video microscopy and migration analyzed by cell tracking
267 software. We first measured migration of Ramos cells plated on a VCAM-1-coated glass surface

268 and stimulated with SDF1 α and found that inhibition of either PI3K γ or PI3K δ impair migration
269 velocity (**Fig S10A**) and mean squared displacement (33), a measure of directional migration
270 persistence (**Fig S10B**). We then assessed migration within a microfluidic device containing an
271 SDF1 α gradient within a collagen gel to allow determination of the chemotactic index, a
272 measure of directional migration reflecting the ability of cells to detect the chemokine gradient
273 (43). Analyses of JVM3 cell migration tracks within this gradient system (**Fig 6A**) revealed that
274 either PI3K δ or PI3K γ inhibition were sufficient to reduce the chemotactic index (**Fig 6B**) and
275 migration velocity (**Fig 6C**) under these conditions, with PI3K γ inhibition showing the strongest
276 effect.

277

278 **PI3K γ or PI3K δ inhibition differentially affect cytoskeletal remodeling and cell** 279 **morphology**

280 We noted that PI3K γ inhibitor-treated cells frequently show abnormal morphologies after SDF1 α
281 stimulation, including dynamic multiple protrusions that fail to develop into fully polarized
282 leading edges (**Fig 7A**). We microscopically scored cells exhibiting round, elongated, polarized
283 or multi-protrusion morphologies by fixing cells after one minute of SDF1 α stimulation and
284 staining the F-actin cytoskeleton (**Fig 7B**). It was found that either PI3K δ or PI3K γ inhibition
285 was sufficient to reduce the proportion of fully polarized cells and increase the proportion of
286 elongated or multi-protrusion morphologies; however, PI3K γ inhibition decreased polarization
287 and increased multi-protrusion morphologies to a greater extent than PI3K δ inhibition (**Fig. 7C**).
288 Together these results indicate a unique and non-redundant role for PI3K γ in mediating
289 chemokine-induced alterations in the cytoskeleton and chemokine gradient sensing.

290

291 **Inhibition of either PI3K γ or PI3K δ significantly decreases the adhesion of CLL cells to**
292 **bone marrow-derived stromal cells**

293 Adhesion of CLL cells to stromal cells is driven by chemokines such as SDF1 α and promotes
294 their retention and interaction with other cell types present in the lymphoid tissue
295 microenvironment (2, 32). To determine the roles of PI3K γ and PI3K δ in the interaction of CLL
296 cells and stromal cells, we co-cultured CLL cells with human stromal cell line HS-5 with or
297 without specific PI3K inhibitors. After 24h, the non-adhered CLL cells were collected and then
298 adhered cells along with the stromal cells were removed using trypsin. CD19-expressing cells in
299 the adhered and non-adhered fractions were counted by flow cytometry and the adhesion index
300 was calculated accordingly. We found that PI3K γ inhibition significantly reduced binding to
301 stromal cells, and dual inhibition of PI3K γ and PI3K δ had a stronger effect than PI3K γ inhibition
302 alone (**Fig 8A**). While basal adhesion to stromal cells was higher in ZAP70⁺ CLL cells as
303 expected, the inhibition of either PI3K γ or PI3K δ significantly decreased CLL cell adhesion in
304 both ZAP70⁺ and ZAP70⁻ groups (**Fig 8B**). In both patient groups, Duvelisib had a stronger
305 effect than either single isoform inhibitor (**Fig 8B**). These differences in response to the
306 inhibitors were not due to differences in cell viability as we did not see noticeable effect of the
307 inhibitors on CLL cell survival under these conditions (**Fig S4**). These results indicate that
308 PI3K γ also contributes to chemokine- and integrin-dependent adhesion of CLL to stromal cells.

309

310

311 **Discussion**

312 The PI 3-kinases α , β , γ and δ collectively regulate major signaling pathways promoting CLL
313 cell chemotaxis, cytoskeletal rearrangement, and CLL cell interaction with the
314 microenvironment. A recent addition to CLL therapy is the PI3K δ -specific inhibitor idelalisib
315 that has shown significant activity in this disease (44). Idelalisib deprives CLL cells of essential
316 survival and proliferative stimuli received from the resident cells of the microenvironment, thus
317 reducing lymphadenopathy and causing egress of CLL cells into peripheral blood. Upon egress,
318 CLL cells may be more vulnerable to the conventional therapeutics used in CLL treatment. We
319 and others have shown that idelalisib can significantly reduce malignant B cell migration in
320 response to chemotactic stimuli (39, 45). Idelalisib was found to affect CLL cell adhesion (32,
321 46) and may also affect tissue-resident cells capacity for cell-cell interaction and secretion of
322 soluble factors (39).

323

324 Unlike protein kinases, all four class I PI3Ks phosphorylate the same target molecules and
325 generate identical D3 phosphoinositide products; thus they are expected to exhibit some
326 functional redundancy. Some level of redundancy may be important to ensure robust activation
327 and fine-tuning of this pathway. One way in which PI3Ks may exhibit unique functions is via
328 differential expression amongst cell types. PI3K δ and PI3K γ subunits are expressed most
329 abundantly in hematologic cells. It was estimated that PI3K δ contributes approximately 50% of
330 the total PI3K activity in lymphocytes (47); thus targeting PI3K δ has a significant impact on
331 lymphocyte functions which are highly dependent on D3 phosphoinositides (48). In contrast, the
332 contributions of PI3K γ have only been clearly defined in T cells and myeloid cells (29, 30, 49).
333 PI3K γ -deficient mice have defective antibody responses upon immunization (30), but this may

334 reflect impaired T cell and myeloid cell function. Moreover, PI3K γ -deficient mouse B cells
335 exhibited normal migration to chemokines in transwell assays and did not show altered homing
336 to tissues when transferred to normal hosts (29), leading to the conclusion that PI3K γ has a
337 minimal role in B cell migration in mice.

338

339 To delineate the respective influence of PI3K δ and PI3K γ in the context of human B cell
340 malignancy, we compared idelalisib to a highly selective PI3K γ inhibitor CZC24832 (33). Both
341 inhibitors were able to significantly reduce CLL migration and adhesion. As these compounds
342 may have differing specificity, potency and stability, we used several approaches to confirm
343 selective effects under the conditions of our experiments. A pan-PI3K inhibitor GDC-0980 was
344 found to have stronger effects on both migration and phosphorylation of Akt and its downstream
345 targets than either PI3K γ , PI3K δ or dual PI3K γ/δ inhibitors. This is consistent with a
346 contribution from PI3K α/β isoforms which is not effectively blocked by PI3K γ/δ inhibitors
347 under the conditions of our experiments. We have also observed that pan-PI3K inhibitor but not
348 PI3K γ inhibitor can block Akt phosphorylation in stromal cells that do not express PI3K γ , further
349 confirming specificity (data not shown). Importantly, we also confirm the key conclusion of the
350 paper regarding PI3K γ and CLL migration using the completely independent approach of genetic
351 silencing by CRISPRi.

352

353 PI3K γ inhibition had a particularly strong effect on directional migration within collagen gels
354 containing an SDF1 α gradient. This suggests an important role of PI3K γ in chemokine sensing
355 and cell polarization towards the chemokine gradient, consistent with findings in neutrophils (23,
356 50, 51). We also found that PI3K γ inhibition had a stronger impact on cell morphology than

357 PI3K δ inhibition, and led to a reduction in polarization and an increase in abnormal multipolar
358 morphologies upon exposure to chemokine. We hypothesize that the direct linkage between
359 PI3K γ and chemokine receptors, via direct p101–G $\beta\gamma$ interactions, provides a unique and
360 indispensable contribution to efficient chemotaxis, perhaps by controlling spatial gradients of
361 phosphoinositides within the plasma membrane. Together these results provide the first
362 demonstration that PI3K γ has unique non-redundant functions in chemokine-mediated responses
363 in human B cell malignancies.

364

365 PI3K γ has two unique adaptor subunits p84 and p101, distinct from the p85 adaptor used by
366 PI3K δ (52). Whereas p84 specifically couples PI3K γ to signaling pathways controlling oxidative
367 burst in neutrophils (23, 50), p101 can directly couple PI3K γ to G $\beta\gamma$ subunits generated by
368 ligand-activated chemokine receptors (53, 54). We found that CLL cells express p101 but not
369 p84 (data not shown). Both p101 and p110 γ catalytic subunits showed increased expression
370 upon activation by CD40L/IL-4 in most CLL patient samples. Consistent with these in vitro data,
371 examination of p101 and p110 γ expression in a well annotated microarray dataset (40) showed
372 that CLL cells isolated from lymph node express higher levels of PI3K γ subunits than CLL cells
373 isolated from blood of the same patients. Moreover, over-expression of p101 and p110 γ together
374 significantly enhanced CLL migration, suggesting that CLL cell expression of functional PI3K γ
375 can be modulated by microenvironmental signals and can functionally impact chemokine
376 receptor-mediated responses.

377

378 Studies in mouse and human have revealed multiple roles of PI3K γ in immune functions.
379 Animals genetically deficient in PI3K γ do not show obvious defects in B cell function, however

380 these mice may have developed compensatory mechanisms such as increased expression of other
381 PI3K isoforms that obscure changes in B cell functions. Moreover, B1 and marginal zone B cells,
382 considered as possible normal counterparts of CLL cells, were not examined in PI3K γ -deficient
383 mice. It remains possible that human B cells are more dependent on PI3K γ than mouse B cells,
384 or that our findings here may reflect unique properties of B cell malignancies. It is established
385 that PI3K γ plays essential roles in normal T, NK and myeloid cell functions in mice (55). As a
386 result, PI3K γ inhibition or dual PI3K δ and PI3K γ inhibition had anti-inflammatory activities in
387 several disease models in mice, attributed to inhibition of cell migration into inflamed tissues
388 (55, 56). Since one of the major hurdles in clinical use of idelalisib is T cell-mediated toxicities
389 (57, 58), it's tempting to speculate that dual inhibition of PI3K δ and PI3K γ may partly mitigate
390 these toxicities by impairing T cell migration into sites of inflammation such as colon, lung or
391 liver.

392

393 Dual inhibition of PI3K δ and PI3K γ has been proposed to have potential benefit for CLL
394 treatment and is currently in clinical trials (39, 59-60). However a direct comparison of the
395 relative effectiveness of dual versus single inhibition has not been reported. We find that dual
396 inhibition has a stronger effect on PI3K/Akt pathway activity, chemokine-dependent migration
397 and adhesion than either PI3K δ or PI3K γ inhibitors. While our findings do not exclude the
398 contribution of other PI3K isoforms, they do provide the first demonstration of a distinct
399 biological function of PI3K γ in B cells. Additional blockade PI3K γ may thus improve clinical
400 benefits via increased anti-leukemic activity and reduced T cell-mediated toxicities.

401

402 **Acknowledgements**

403 Funding for this work was provided by a grant from the Leukemia and Lymphoma Society of
404 Canada to AJM, SBG and FL. AJM was supported by a Canada Research Chair. AYA was
405 supported by a fellowship from CancerCare Manitoba and Research Manitoba. XW was
406 supported by a studentship from Research Manitoba and NE by the Children's Hospital Research
407 Institute of Manitoba. JEG was supported by Natural Sciences and Engineering Research
408 Council of Canada and the Canada Foundation for Innovation. TTM was supported by the GSK-
409 CIHR Partnered program and Research Manitoba. The CLL research cluster and tumor bank
410 were supported by Research Manitoba and CancerCare Manitoba. The authors would like to
411 thank Christine Zhang for technical support, Donna Hewitt, Michelle Queau, Mandy Squires,
412 Yun Li, Laurie Lange and all the Manitoba Blood and Marrow bank staff for management of
413 patient samples and clinical information, and the patients for their blood donations.

414

415 **Author contributions**

416 AYA and XW performed research, analyzed data, performed statistical analyses and wrote the
417 manuscript. NE, SH, and JEG performed research. VB and JBJ designed research and collected
418 vital biomarker and clinical data. FL and TTM contributed vital analytical tools. SBG designed
419 research and analyzed and interpreted data. AJM designed research, analyzed and interpreted
420 data, supervised trainees and wrote the manuscript.

421

422 **Conflict of interest disclosures**

423 The authors have no conflict of interest to declare.

424

425 **References**

- 426
- 427 1. Stevenson FK, Krysov S, Davies AJ, Steele AJ, Packham G. B-cell receptor signaling in chronic
428 lymphocytic leukemia. *Blood*. 2011;118(16):4313-20.
- 429 2. Burger JA, Gribben JG. The microenvironment in chronic lymphocytic leukemia (CLL) and other B
430 cell malignancies: insight into disease biology and new targeted therapies. *Semin Cancer Biol*.
431 2014;24:71-81.
- 432 3. Lagneaux L, Delforge A, Bron D, De Bruyn C, Stryckmans P. Chronic lymphocytic leukemic B cells
433 but not normal B cells are rescued from apoptosis by contact with normal bone marrow stromal cells.
434 *Blood*. 1998;91(7):2387-96.
- 435 4. Munk Pedersen I, Reed J. Microenvironmental interactions and survival of CLL B-cells. *Leuk*
436 *Lymphoma*. 2004;45(12):2365-72.
- 437 5. Burger JA, Ghia P, Rosenwald A, Caligaris-Cappio F. The microenvironment in mature B-cell
438 malignancies: a target for new treatment strategies. *Blood*. 2009;114(16):3367-75.
- 439 6. Crespo M, Bosch F, Villamor N, Bellosillo B, Colomer D, Rozman M, et al. ZAP-70 expression as a
440 surrogate for immunoglobulin-variable-region mutations in chronic lymphocytic leukemia. *N Engl J Med*.
441 2003;348(18):1764-75.
- 442 7. Preobrazhensky SN, Szankasi P, Bahler DW. Improved flow cytometric detection of ZAP-70 in
443 chronic lymphocytic leukemia using experimentally optimized isotypic control antibodies. *Cytometry B*
444 *Clin Cytom*. 2012;82(2):78-84.
- 445 8. Durig J, Nuckel H, Cremer M, Fuhrer A, Halfmeyer K, Fandrey J, et al. ZAP-70 expression is a
446 prognostic factor in chronic lymphocytic leukemia. *Leukemia*. 2003;17(12):2426-34.
- 447 9. Stilgenbauer S. Prognostic markers and standard management of chronic lymphocytic leukemia.
448 *Hematology Am Soc Hematol Educ Program*. 2015;2015:368-77.
- 449 10. Deaglio S, Vaisitti T, Aydin S, Bergui L, D'Arena G, Bonello L, et al. CD38 and ZAP-70 are
450 functionally linked and mark CLL cells with high migratory potential. *Blood*. 2007;110(12):4012-21.
- 451 11. Lafarge ST, Li H, Pauls SD, Hou S, Johnston JB, Gibson SB, et al. ZAP70 expression directly
452 promotes chronic lymphocytic leukaemia cell adhesion to bone marrow stromal cells. *Br J Haematol*.
453 2015;168(1):139-42.
- 454 12. Richardson SJ, Matthews C, Catherwood MA, Alexander HD, Carey BS, Farrugia J, et al. ZAP-70
455 expression is associated with enhanced ability to respond to migratory and survival signals in B-cell
456 chronic lymphocytic leukemia (B-CLL). *Blood*. 2006;107(9):3584-92.
- 457 13. Cheng JQ, Godwin AK, Bellacosa A, Taguchi T, Franke TF, Hamilton TC, et al. AKT2, a putative
458 oncogene encoding a member of a subfamily of protein-serine/threonine kinases, is amplified in human
459 ovarian carcinomas. *Proc Natl Acad Sci U S A*. 1992;89(19):9267-71.
- 460 14. Kandel ES, Hay N. The regulation and activities of the multifunctional serine/threonine kinase
461 Akt/PKB. *Exp Cell Res*. 1999;253(1):210-29.
- 462 15. Testa JR, Bellacosa A. AKT plays a central role in tumorigenesis. *Proc Natl Acad Sci U S A*.
463 2001;98(20):10983-5.
- 464 16. Nicholson KM, Anderson NG. The protein kinase B/Akt signalling pathway in human malignancy.
465 *Cell Signal*. 2002;14(5):381-95.
- 466 17. Vivanco I, Sawyers CL. The phosphatidylinositol 3-Kinase AKT pathway in human cancer. *Nat Rev*
467 *Cancer*. 2002;2(7):489-501.
- 468 18. Brown JR, Byrd JC, Coutre SE, Benson DM, Flinn IW, Wagner-Johnston ND, et al. Idelalisib, an
469 inhibitor of phosphatidylinositol 3-kinase p110delta, for relapsed/refractory chronic lymphocytic
470 leukemia. *Blood*. 2014;123(22):3390-7.

- 471 19. Wei M, Wang X, Song Z, Jiao M, Ding J, Meng LH, et al. Targeting PI3Kdelta: emerging therapy
472 for chronic lymphocytic leukemia and beyond. *Med Res Rev.* 2015;35(4):720-52.
- 473 20. Till KJ, Pettitt AR, Slupsky JR. Expression of functional sphingosine-1 phosphate receptor-1 is
474 reduced by B cell receptor signaling and increased by inhibition of PI3 kinase delta but not SYK or BTK in
475 chronic lymphocytic leukemia cells. *J Immunol.* 2015;194(5):2439-46.
- 476 21. Barrientos JC. Idelalisib for the treatment of chronic lymphocytic leukemia/small lymphocytic
477 lymphoma. *Future Oncol.* 2016;12(18):2077-94.
- 478 22. Bohnacker T, Marone R, Collmann E, Calvez R, Hirsch E, Wymann MP. PI3Kgamma adaptor
479 subunits define coupling to degranulation and cell motility by distinct PtdIns(3,4,5)P3 pools in mast cells.
480 *Sci Signal.* 2009;2(74):ra27.
- 481 23. Deladeriere A, Gambardella L, Pan D, Anderson KE, Hawkins PT, Stephens LR. The regulatory
482 subunits of PI3Kgamma control distinct neutrophil responses. *Sci Signal.* 2015;8(360):ra8.
- 483 24. Brazzatti JA, Klingler-Hoffmann M, Haylock-Jacobs S, Harata-Lee Y, Niu M, Higgins MD, et al.
484 Differential roles for the p101 and p84 regulatory subunits of PI3Kgamma in tumor growth and
485 metastasis. *Oncogene.* 2012;31(18):2350-61.
- 486 25. Vadas O, Dbouk HA, Shymanets A, Perisic O, Burke JE, Abi Saab WF, et al. Molecular
487 determinants of PI3Kgamma-mediated activation downstream of G-protein-coupled receptors (GPCRs).
488 *Proc Natl Acad Sci U S A.* 2013;110(47):18862-7.
- 489 26. Turvey ME, Klingler-Hoffmann M, Hoffmann P, McColl SR. p84 forms a negative regulatory
490 complex with p110gamma to control PI3Kgamma signalling during cell migration. *Immunol Cell Biol.*
491 2015;93(8):735-43.
- 492 27. Thomas MS, Mitchell JS, DeNucci CC, Martin AL, Shimizu Y. The p110gamma isoform of
493 phosphatidylinositol 3-kinase regulates migration of effector CD4 T lymphocytes into peripheral
494 inflammatory sites. *J Leukoc Biol.* 2008;84(3):814-23.
- 495 28. Martin AL, Schwartz MD, Jameson SC, Shimizu Y. Selective regulation of CD8 effector T cell
496 migration by the p110 gamma isoform of phosphatidylinositol 3-kinase. *J Immunol.* 2008;180(4):2081-8.
- 497 29. Reif K, Okkenhaug K, Sasaki T, Penninger JM, Vanhaesebroeck B, Cyster JG. Cutting edge:
498 differential roles for phosphoinositide 3-kinases, p110gamma and p110delta, in lymphocyte chemotaxis
499 and homing. *J Immunol.* 2004;173(4):2236-40.
- 500 30. Sasaki T, Irie-Sasaki J, Jones RG, Oliveira-dos-Santos AJ, Stanford WL, Bolon B, et al. Function of
501 PI3Kgamma in thymocyte development, T cell activation, and neutrophil migration. *Science.*
502 2000;287(5455):1040-6.
- 503 31. Dong S, Guinn D, Dubovsky JA, Zhong Y, Lehman A, Kutok J, et al. IPI-145 antagonizes intrinsic
504 and extrinsic survival signals in chronic lymphocytic leukemia cells. *Blood.* 2014;124(24):3583-6.
- 505 32. Lafarge ST, Johnston JB, Gibson SB, Marshall AJ. Adhesion of ZAP-70+ chronic lymphocytic
506 leukemia cells to stromal cells is enhanced by cytokines and blocked by inhibitors of the PI3-kinase
507 pathway. *Leuk Res.* 2014;38(1):109-15.
- 508 33. Bergamini G, Bell K, Shimamura S, Werner T, Cansfield A, Muller K, et al. A selective inhibitor
509 reveals PI3Kgamma dependence of T(H)17 cell differentiation. *Nat Chem Biol.* 2012;8(6):576-82.
- 510 34. Ali AY, Abedini MR, Tsang BK. The oncogenic phosphatase PPM1D confers cisplatin resistance in
511 ovarian carcinoma cells by attenuating checkpoint kinase 1 and p53 activation. *Oncogene.*
512 2012;31(17):2175-86.
- 513 35. Eissa N, Hussein H, Wang H, Rabbi MF, Bernstein CN, Ghia JE. Stability of Reference Genes for
514 Messenger RNA Quantification by Real-Time PCR in Mouse Dextran Sodium Sulfate Experimental Colitis.
515 *PLoS One.* 2016;11(5):e0156289.
- 516 36. Gilbert LA, Horlbeck MA, Adamson B, Villalta JE, Chen Y, Whitehead EH, et al. Genome-Scale
517 CRISPR-Mediated Control of Gene Repression and Activation. *Cell.* 2014;159(3):647-61.

518 37. Li H, Hou S, Wu X, Nandagopal S, Lin F, Kung S, et al. The tandem PH domain-containing protein
519 2 (TAPP2) regulates chemokine-induced cytoskeletal reorganization and malignant B cell migration. *PLoS*
520 *One*. 2013;8(2):e57809.

521 38. Foley MH, Forcier T, McAndrew E, Gonzalez M, Chen H, Juelg B, et al. High Avidity CD8(+) T Cells
522 Efficiently Eliminate Motile HIV-Infected Targets and Execute a Locally Focused Program of Anti-Viral
523 Function. *PLoS ONE*. 2014;9(2):e87873.

524 39. Hoellenriegel J, Meadows SA, Sivina M, Wierda WG, Kantarjian H, Keating MJ, et al. The
525 phosphoinositide 3'-kinase delta inhibitor, CAL-101, inhibits B-cell receptor signaling and chemokine
526 networks in chronic lymphocytic leukemia. *Blood*. 2011;118(13):3603-12.

527 40. Herishanu Y, Perez-Galan P, Liu D, Biancotto A, Pittaluga S, Vire B, et al. The lymph node
528 microenvironment promotes B-cell receptor signaling, NF-kappaB activation, and tumor proliferation in
529 chronic lymphocytic leukemia. *Blood*. 2011;117(2):563-74.

530 41. Suire S, Condliffe AM, Ferguson GJ, Ellson CD, Guillou H, Davidson K, et al. Gbetagammagamma and
531 the Ras binding domain of p110gamma are both important regulators of PI(3)Kgamma signalling in
532 neutrophils. *Nat Cell Biol*. 2006;8(11):1303-9.

533 42. Nombela-Arrieta C, Lacalle RA, Montoya MC, Kunisaki Y, Megias D, Marques M, et al. Differential
534 requirements for DOCK2 and phosphoinositide-3-kinase gamma during T and B lymphocyte homing.
535 *Immunity*. 2004;21(3):429-41.

536 43. Beltman JB, Maree AFM, de Boer RJ. Analysing immune cell migration. *Nat Rev Immunol*.
537 2009;9(11):789-98.

538 44. Furman RR, Sharman JP, Coutre SE, Cheson BD, Pagel JM, Hillmen P, et al. Idelalisib and
539 rituximab in relapsed chronic lymphocytic leukemia. *N Engl J Med*. 2014;370(11):997-1007.

540 45. Dubovsky JA, Chappell DL, Harrington BK, Agrawal K, Andritsos LA, Flynn JM, et al. Lymphocyte
541 cytosolic protein 1 is a chronic lymphocytic leukemia membrane-associated antigen critical to niche
542 homing. *Blood*. 2013;122(19):3308-16.

543 46. Fiorcari S, Brown WS, McIntyre BW, Estrov Z, Maffei R, O'Brien S, et al. The PI3-kinase delta
544 inhibitor idelalisib (GS-1101) targets integrin-mediated adhesion of chronic lymphocytic leukemia (CLL)
545 cell to endothelial and marrow stromal cells. *PLoS One*. 2013;8(12):e83830.

546 47. Okkenhaug K, Bilancio A, Farjot G, Priddle H, Sancho S, Peskett E, et al. Impaired B and T cell
547 antigen receptor signaling in p110delta PI 3-kinase mutant mice. *Science*. 2002;297(5583):1031-4.

548 48. So L, Fruman DA. PI3K signalling in B- and T-lymphocytes: new developments and therapeutic
549 advances. *Biochem J*. 2012;442(3):465-81.

550 49. Hirsch E, Katanaev VL, Garlanda C, Azzolino O, Pirola L, Silengo L, et al. Central role for G protein-
551 coupled phosphoinositide 3-kinase gamma in inflammation. *Science*. 2000;287(5455):1049-53.

552 50. Hannigan M, Zhan L, Li Z, Ai Y, Wu D, Huang CK. Neutrophils lacking phosphoinositide 3-kinase
553 gamma show loss of directionality during N-formyl-Met-Leu-Phe-induced chemotaxis. *Proc Natl Acad Sci*
554 *U S A*. 2002;99(6):3603-8.

555 51. Van Haastert PJ, Devreotes PN. Chemotaxis: signalling the way forward. *Nat Rev Mol Cell Biol*.
556 2004;5(8):626-34.

557 52. Shymanets A, Prajwal, Bucher K, Beer-Hammer S, Harteneck C, Nurnberg B. p87 and p101
558 subunits are distinct regulators determining class IB phosphoinositide 3-kinase (PI3K) specificity. *J Biol*
559 *Chem*. 2013;288(43):31059-68.

560 53. Brock C, Schaefer M, Reusch HP, Czupalla C, Michalke M, Spicher K, et al. Roles of G beta gamma
561 in membrane recruitment and activation of p110 gamma/p101 phosphoinositide 3-kinase gamma. *J Cell*
562 *Biol*. 2003;160(1):89-99.

563 54. Kurig B, Shymanets A, Bohnacker T, Prajwal, Brock C, Ahmadian MR, et al. Ras is an
564 indispensable coregulator of the class IB phosphoinositide 3-kinase p87/p110gamma. *Proc Natl Acad Sci*
565 *U S A*. 2009;106(48):20312-7.

- 566 55. Rommel C. Taking PI3Kdelta and PI3Kgamma one step ahead: dual active PI3Kdelta/gamma
567 inhibitors for the treatment of immune-mediated inflammatory diseases. *Curr Top Microbiol Immunol.*
568 2010;346:279-99.
- 569 56. Winkler DG, Faia KL, DiNitto JP, Ali JA, White KF, Brophy EE, et al. PI3K-delta and PI3K-gamma
570 inhibition by IPI-145 abrogates immune responses and suppresses activity in autoimmune and
571 inflammatory disease models. *Chem Biol.* 2013;20(11):1364-74.
- 572 57. Brown JR. The PI3K pathway: clinical inhibition in chronic lymphocytic leukemia. *Semin Oncol.*
573 2016;43(2):260-4.
- 574 58. Jones JA, Robak T, Brown JR, Awan FT, Badoux X, Coutre S, et al. Efficacy and safety of idelalisib
575 in combination with ofatumumab for previously treated chronic lymphocytic leukaemia: an open-label,
576 randomised phase 3 trial. *Lancet Haematol.* 2017;4(3):e114-e26.
- 577 59. Gockeritz E, Kerwien S, Baumann M, Wigger M, Vondey V, Neumann L, et al. Efficacy of
578 phosphatidylinositol-3 kinase inhibitors with diverse isoform selectivity profiles for inhibiting the survival
579 of chronic lymphocytic leukemia cells. *Int J Cancer.* 2015;137(9):2234-42.
- 580 60. Balakrishnan K, Peluso M, Fu M, Rosin NY, Burger JA, Wierda WG, et al. The phosphoinositide-3-
581 kinase (PI3K)-delta and gamma inhibitor, IPI-145 (Duvelisib), overcomes signals from the PI3K/AKT/S6
582 pathway and promotes apoptosis in CLL. *Leukemia.* 2015;29(9):1811-22.
- 583

584

585 **Figure Legends**

586

587 **Figure 1: Inhibition of PI3K γ impairs Akt phosphorylation and B cell migration in**
588 **transwell assay.**

589 **(A)** Inhibition of PI3K γ or PI3K δ significantly decreased the migration of JVM3 cells. JVM3
590 cells were cultured in medium or stimulated for 24h with CD40L/IL-4 and then incubated with
591 the PI3K γ -specific inhibitor CZC24832 (2 μ M), the PI3K δ -specific inhibitor idelalisib (1 μ M),
592 dual PI3K δ/γ inhibitor duvelisib (1 μ M), or the PI3K pan inhibitor GDC0980 (1 μ M) and
593 subjected to a transwell migration assay. DMSO served as the vehicle control for the inhibitors
594 while SDF1 α (100 ng/ml) served as the chemoattractant (n=7). **(B)** Effect of PI3K γ inhibitor on
595 Akt phosphorylation. JVM3 cells were pre-incubated with indicated concentrations of CZC4832
596 (in μ M) and then stimulated with SDF1 α for 10 min. Akt Ser473 phosphorylation and total Akt
597 levels were assessed by Western blot.

598

599 **Figure 2: Inhibition of PI3K γ or PI3K δ impairs CLL cell migration.**

600 **(A)** Effect of PI3K γ inhibitor on CLL migration. CLL cells were cultured in medium or
601 stimulated with CD40L+IL-4 for 24h and subjected to a transwell migration assay. Graphs
602 represent migration of individual CLL patient samples with or without addition of PI3K γ
603 inhibitor CZC24832, connected by lines. **(B)** Inhibition of PI3K γ or PI3K δ decreases the
604 migration of CLL cells to a similar extent, while dual PI3K γ/δ inhibition using duvelisib has
605 significantly greater effect than PI3K γ inhibitor alone. **(C)** Combination of PI3K γ inhibitor and
606 PI3K δ inhibitor decreases the migration of CLL cells to a greater extent than either inhibitor
607 alone. Lines connect individual patient migration responses in the presence of the indicated

608 inhibitors. Note all inhibitor-treated groups were significantly different than the control
609 untreated group, whereas the CZC24832+idelalisib combination was not significantly different
610 than duvelisib. Significance was determined as determined using paired T-tests * $p < 0.05$, ** p
611 < 0.01 , *** $p < 0.001$.

612

613 **Figure 3: The effect of CRISPRi knockdown of p110 γ on the migration of malignant B cell**
614 **lines and CLL cells.**

615 (A) Confirmation of p110 γ CRISPRi knockdown specificity. JVM3 cells were transfected with
616 either dCas-GFP expression vector alone (Control) or co-transfected with dCas9-GFP plus
617 vectors expressing p110 γ -targeting guide RNAs (at a 1:3 ratio). After 24h, p110 isoform
618 expression within sorted GFP+ transfectants was assessed by qPCR. (B) p110 γ knockdown
619 significantly impaired the migration of JVM3 and Ramos cells. Cells were transfected as above
620 and then subjected to a transwell migration assay. Data represent average fold change in
621 migration of GFP+ cells (n = 3). (C) p110 γ knockdown significantly reduced the migration of
622 primary CLL cells regardless of their IgVH mutation status. CLL cells were transfected with
623 either dCas-GFP expression vector or dCas9-GFP plus vectors expressing p110 γ -targeting guide
624 RNAs then assessed 48h later using a transwell migration assay. Percent of cells migrating
625 toward SDF1 α was determined by flow cytometry counting of live GFP-expressing cells present
626 in upper and lower chambers after 3h.

627

628 **Figure 4: Expression of PI3K γ subunits in malignant B cell lines and CLL patient samples.**

629 (A/B) CLL cells were stimulated with F(ab')₂ α -IgM (10 μ g/ml) or CD40L/IL-4 (50 ng/ml each)
630 and harvested 24h later for RNA extraction and RT-qPCR analysis. mRNA expression of (A)

631 p110 γ and **(B)** p101 were determined, and expression levels were normalized against expression
632 of TATA box binding protein (*TBP*). Patients were divided into indolent versus progressive
633 groups based on IgVH mutation status. **(C)** Protein expression of p110 γ and p101 in CLL
634 samples in response to BCR stimulation or CD40L/IL-4 stimulation. Data are representative of 9
635 patients analyzed.

636

637 **Figure 5: Over-expression of PI3K γ subunits affects the migration of malignant B cells.**

638 **(A)** Confirmation of p110 γ -GFP and p101-GFP overexpression in JVM3 cells. JVM3 cells were
639 transfected with either p101-GFP or p110 γ -GFP plasmids. 24h post transfection, RNA was
640 harvested and expression of p101 or p110 γ was determined by RT-qPCR analysis. **(B)**
641 Overexpression of p110 γ or p101 enhances the migration of JVM3 in response to the chemokine
642 SDF1 α . 24h after transfection with p101-GFP plasmid or p110 γ -GFP, migration of live GFP-
643 expressing cells in response to SDF1 α (100 ng/ml) was assessed using a transwell migration
644 assay. The graph shows the mean and SEM of four experiments. **(C)** Overexpression of PI3K γ
645 subunits enhances CLL cell migration. p110 γ -GFP, p101-GFP, or both together were over-
646 expressed in CLL cells. After 48 h, migration of live GFP+ cells was assessed by transwell
647 assay as above. Results are expressed as fold change in migration relative to the control
648 transfection of the same patient sample.

649

650 **Figure 6: Impact of PI3K γ or PI3K δ inhibition on directional migration behavior.**

651 JVM3 cells were seeded into a collagen gel and treated with indicated inhibitors for 60 minutes.
652 After establishing the SDF1 α gradient, time-lapse imaging was performed and cell migration
653 tracks were analyzed using IMARIS software. **(A)** Plots illustrate cell tracks from a single

654 representative experiment, overlaid to the same origin. Note that cells treated with CZC24843
655 show visibly impaired chemotaxis towards the higher SDF1 α concentration (right half of the
656 graphs). **(B-C)** Quantitative analysis of cell tracks showing that both PI3K δ and PI3K γ inhibition
657 reduced the chemotactic index **(B)** and migration velocity **(C)**. Mann-Whitney test, ** $p < 0.01$;
658 *** $p < 0.001$.

659

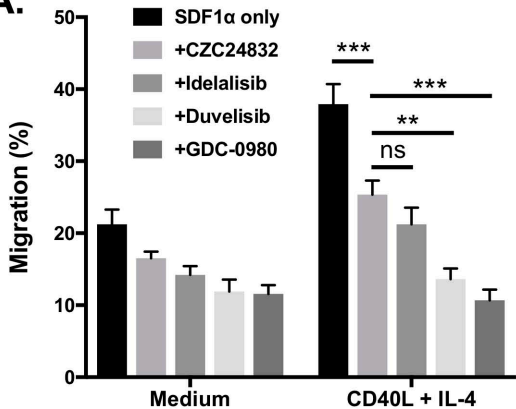
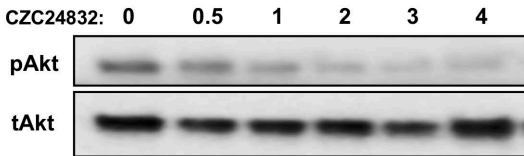
660 **Figure 7: PI3K δ and PI3K γ inhibitors differentially affect cytoskeletal remodeling and cell**
661 **morphology.**

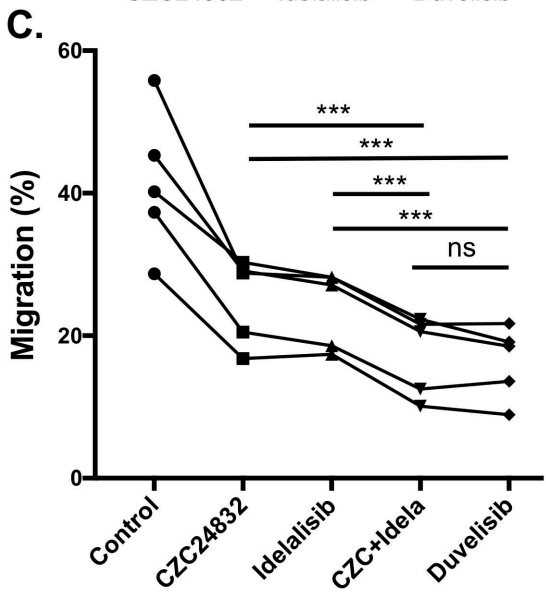
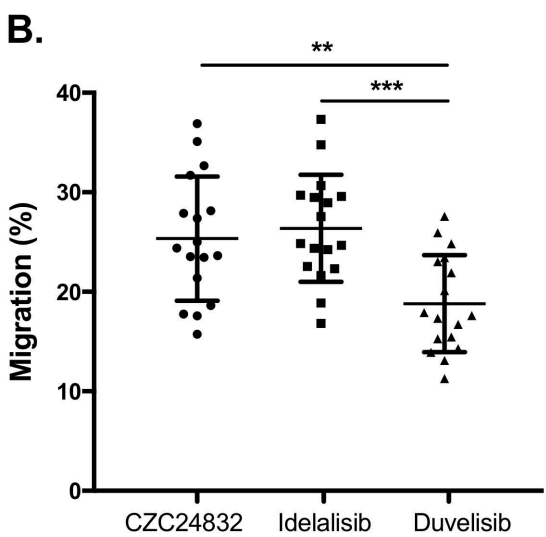
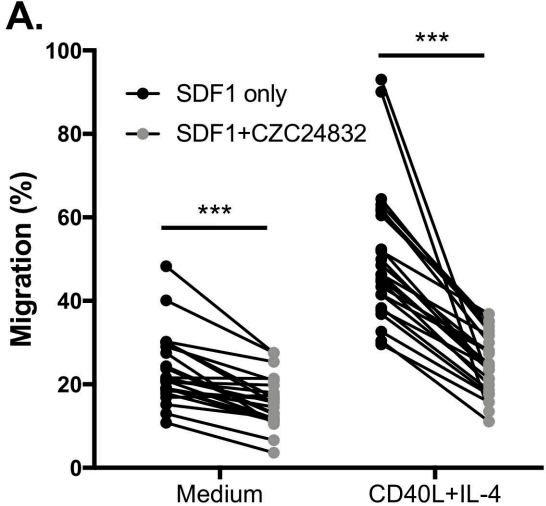
662 **(A)** Time-lapse images of CZC24832-treated Ramos cells migrating within SDF1 α gradient,
663 showing the dynamic formation and retraction of multiple protrusions and failure to form stable
664 polarized morphology. Note that all three cells in this field exhibit multiple protrusions at one of
665 the time points (indicated by arrows) and failed to migrate significantly in the direction of the
666 SDF1 gradient. **(B)** Morphological scoring demonstrating the differential impact of PI3K δ and
667 PI3K γ inhibitors on Ramos cell polarization. Ramos cells were pretreated with inhibitors,
668 stimulated with 100 ng/ml SDF1 α for 1 min, then fixed and F-actin stained using Alexa-488
669 phalloidin. Representative CZC24832-treated cells exhibiting the four major observed
670 morphologies are shown. **(C)** Frequency of cells exhibiting each morphology within control and
671 inhibitor-treated groups. Data are based on 3 independent experiments scoring over 200 cells per
672 treatment group in total. Paired T test, * denotes significance comparing drug-treated to control,
673 + denotes significance comparing CZC24832 to Idelalisib.

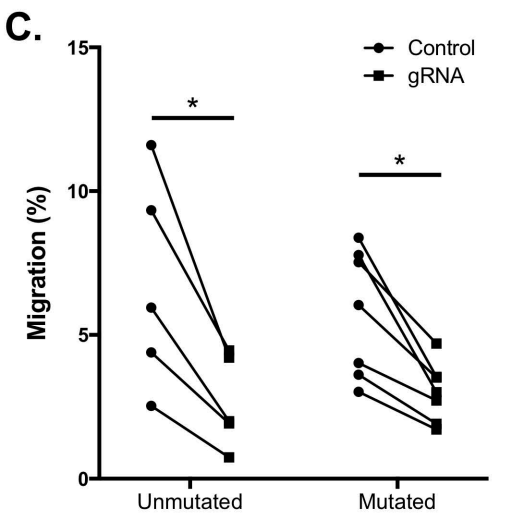
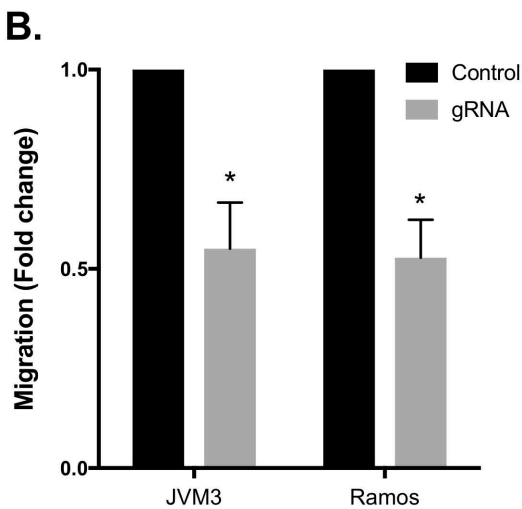
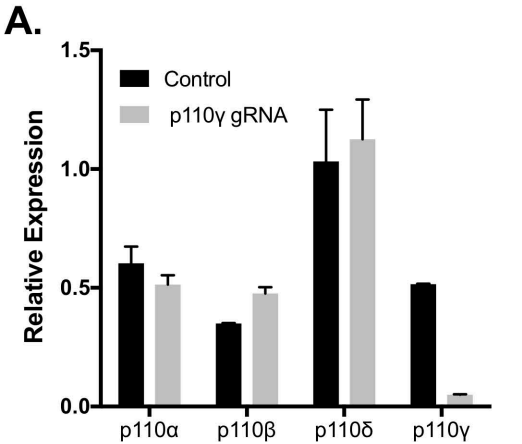
674

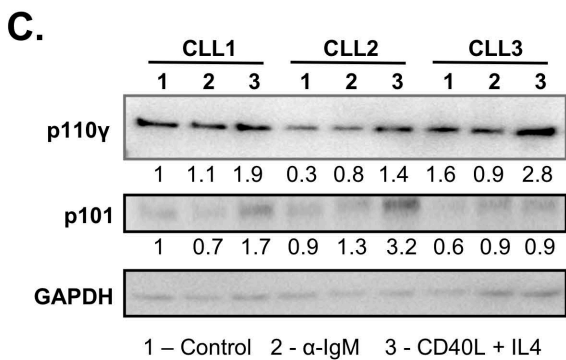
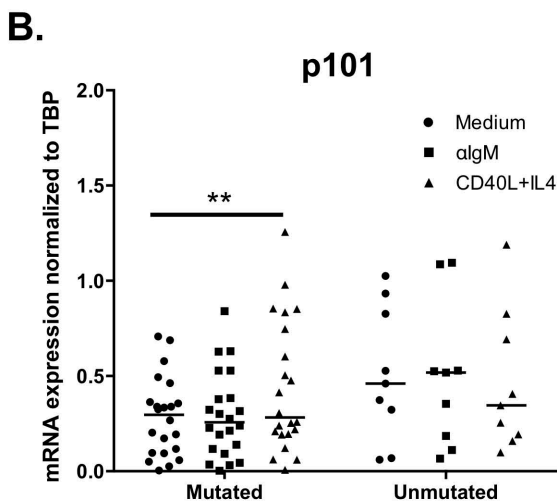
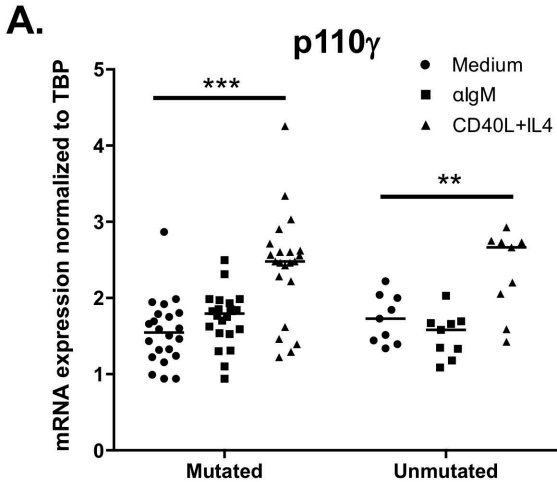
675 **Figure 8: Inhibition of either PI3K γ or PI3K δ significantly decreases the adhesion of CLL**
676 **cells to stromal cells without affecting CLL cell survival**

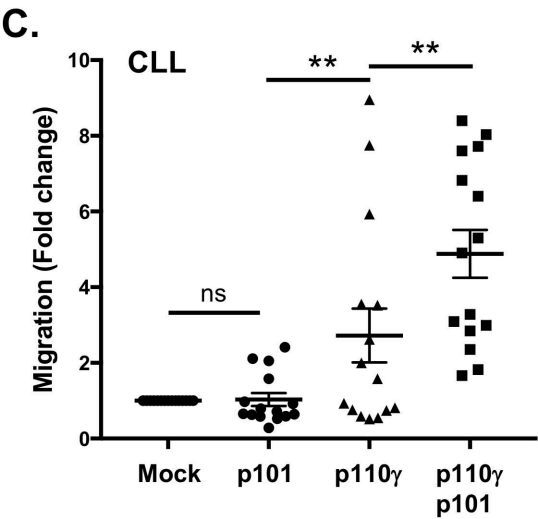
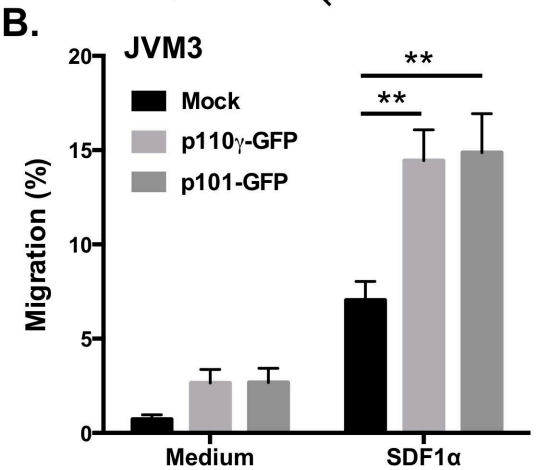
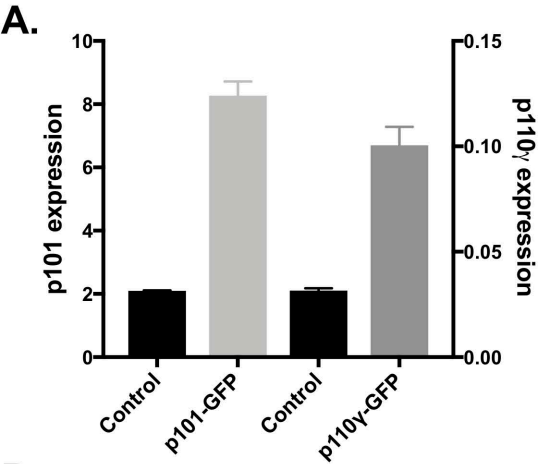
677 CLL cells were incubated for 24h with established monolayers of human stromal cell line HS-5
678 in the presence of the indicated inhibitors. The adhered and non-adhered CLL cell fractions were
679 counted by flow cytometry, gating on the live cell population expressing CD19, to determine the
680 percent adhesion **(A)** Impact of PI3K γ or PI3K γ /PI3K δ dual inhibitors on stromal cell binding.
681 The graph displays percent adhesion of individual CLL patient samples under different inhibitor
682 treatment conditions. Inhibition of PI3K γ or PI3K δ significantly decreased the adhesion of CLL
683 cells regardless of **(B)** ZAP70 status or **(C)** IgVH mutation status.
684

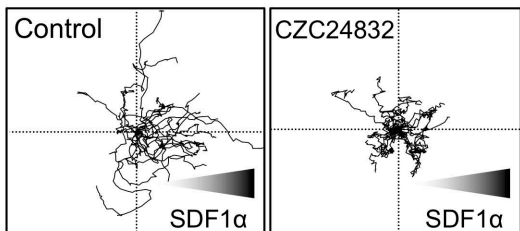
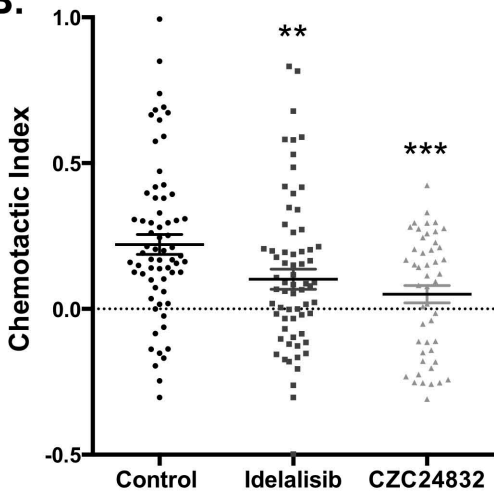
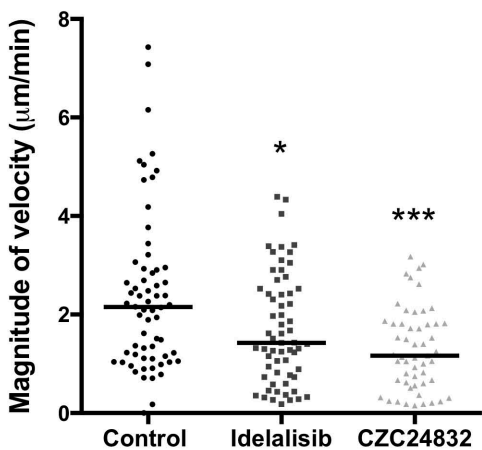
A.**B.**

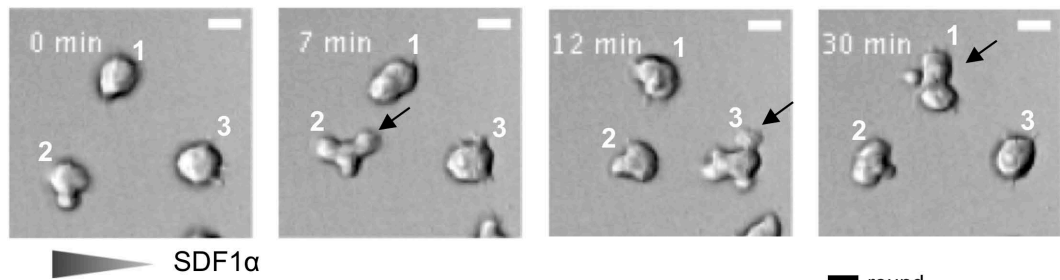
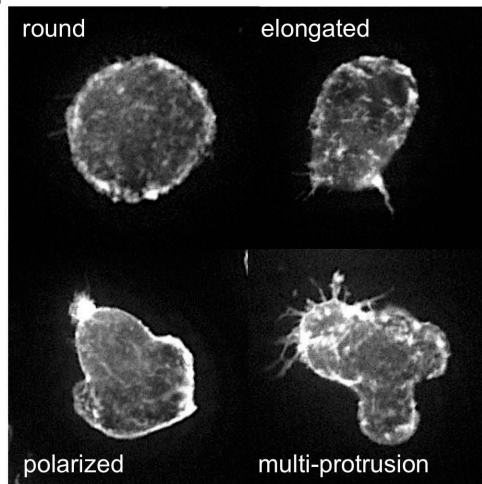








A.**B.****C.**

A.**B.****C.**